

## Formation of the composition and characteristics of the surface of chromonickel steel 12CR18NI10T during laser modification in a layer of experimental alloying coating

© V.I. Proskuryakov, I.V. Rodionov

Yuri Gagarin State Technical University of Saratov, Saratov, Russia  
e-mail: prosku.94@mail.ru

Received June 7, 2021

Revised October 4, 2021

Accepted October 5, 2021

The results of an experimental study of laser pulsed modification of the surface of stainless steel 12CR18NI10T in a layer of alloying compound made of graphite paste and nanodispersed titanium dioxide powder (anatase) and without coating are presented. A comparative analysis of the effect of the coating on the elemental and phase compositions, morphological characteristics and microhardness of the modified surface is carried out. It was found that as a result of the treatment, the processes of cementation and oxidation of the surface occur, which made it possible to obtain a mixture of iron carbide and high-strength oxides in the surface layer of steel. In the samples that underwent laser treatment in the coating layer, an increase in the intensity of the diffraction peaks of the graphite phase and the formation of iron oxides  $Fe_3O_4$  and chromium  $Cr_2O_3$  with the presence of titanium dioxide  $TiO_2$  were revealed, which created a mixed heterophase metal oxide structure with increased mechanical strength. An increase in the microhardness of the modified surface after laser pulsed scanning in the layer of the experimental alloying compound is established.

**Keywords:** Stainless steel, laser modification, alloying coating, elemental and phase compositions, surface structure, microhardness.

DOI: 10.21883/TP.2022.01.52534.173-21

### Introduction

Laser processing is currently used alongside the classical thermal and thermochemical processing for hardening the surface layer of metals and alloys. The key advantages of this technique are the locality and reproducibility of processing, speed, and low energy consumption achieved due to the simplicity of adjustment of the heat release in the treated zone through variation of the energy and duration of pulses [1–3].

The processes of surface alloying with various suspensions, pastes, and alloying coatings are being developed actively in laser technology. Compared to the traditional methods of thermochemical processing, laser alloying in a coating layer expands the spectrum of possible structures of alloyed layers. The chemical composition of a layer and its microhardness and homogeneity may be adjusted by varying the following key processing parameters: type and thickness of the alloying coating, fractional composition of the powder used, type of the ambient gas, geometry of focusing of laser radiation, and beam power and scanning speed [4–7].

It is known that the martensitic structure forming in the melt zone upon laser hardening of stainless steel becomes more disperse as the processing rate increases. In addition, the atmosphere type has an effect on both the geometric sizes of alloyed zones and on the degree of dispersion of the formed structure. If processing is performed with a small focal spot and with the use of argon, a needle-like

or microglobular martensitic structure forms (depending on the type of the alloying component) at standard processing rates. The microhardness in the alloyed zone may be as high as 13 000–18 000 MPa. The presence of such defects as pores and cracks in the alloyed zone may be excluded completely [8].

T. Yamaguchi have reported on the process of laser alloying of austenitic stainless steel AISI 304 (corresponds to steel 08Cr18Ni10) with a light-transmitting resin used as a source for the carbon element. It was found that titanium carbide was distributed uniformly within the pool in processing with a moderate-power laser, and the hardness of the alloyed zone increased to approximately 1200 HV. When the average laser power was increased, the intermetallic  $\beta$  phase formed, and the surface cracked as a result [9]. F. Laroudie et al. have established that the surface hardness of stainless steel 316L (corresponds to 08Cr16Ni11Mo3) subjected to laser alloying with a titanium carbide powder was approximately equal to 280 HV [10]. Since the majority of titanium carbide was in this case concentrated in large clusters, the hardness outside clusters increased only slightly. B. AlMangour et al. have produced TiC-reinforced 316L stainless steel composites by selective laser melting [11]. The hardness of these composites was approximately equal to 400 HV and was affected significantly by the size of grains of titanium carbide and the density of composites.

Methods of modification of the surface of stainless steel AISI 316 (corresponds to 03Cr17Ni14Mo3) with a

continuous-wave CO<sub>2</sub> laser with a power up to 4 kW at different scanning rates are known. It was found that pre-coating of the steel surface with graphite powder and subsequent laser processing resulted in a change in the microstructure, which consisted of  $\gamma$  dendrite surrounded by a network of eutectic structures ( $\gamma$  + carbide), and an increase in microhardness, which reached 500 HV. The corrosion resistance was also improved considerably compared to the initial unmodified surface [12].

The method of laser modification of stainless steel X12CrNiMo with the introduction of a mixture of titanium carbide powder and powder of a solid cobalt-based Stellite 6 alloy into the treated zone (with varying percentage ratios of alloying components) warrants particular attention. This processing was performed using a 4.4 kW continuous-wave YAG laser. The microhardness of the surface alloyed with titanium carbide was found to be as high as 600 HV. With a mixture of 30% of Stellite 6 powder and 70% of titanium carbide, the microhardness could reach 1025 HV [13].

However, despite scientific and practical interest, the application of laser pulsed alloying is currently limited, and this technology remains in the early phase of development and implementation. The reason for this is the insufficient knowledge of the patterns of variation of properties of processed metals and alloys in relation to the phase and structural state formed under laser alloying with different materials at high heating and cooling rates. This lack of information hinders the development of process technologies and recommendations. In addition, the discussed method has a disadvantage in that pores, holes, and splashes form as alloying materials (especially gaseous ones) are introduced into the molten pool [14,15].

The key studied parameters of the surface modified by laser pulsed alloying of stainless chromium-nickel steel articles are as follows: morphological characteristics, elemental and phase composition, structural state of the scanned layer, and its microhardness. The estimation of parameters of exposure of a steel surface with an alloying coating to laser pulsed radiation should provide an opportunity to formulate the conditions required to form modified layers with enhanced physical and mechanical properties.

In view of the above, the present study was focused on establishing the effect of laser alloying of stainless steel with an experimental alloying coating consisting of graphite paste and anatase titania TiO<sub>2</sub> powder on the chemical and phase composition, the morphology, and the microhardness of the modified surface. The obtained results allowed us to determine the effect of coating on the process of formation of a cemented layer and on the alteration of the phase and structural state of the surface after laser pulsed scanning.

## 1. Experimental procedure

The test samples were plates 10 × 10 mm in size and 3 mm in thickness. Stainless chromium-nickel steel 12Cr18Ni10Ti (GOST 5632-2014) was the studied material.

The surface of samples was prepared in several laboratory stages prior to laser pulsed alloying. At the first stage, air-powder abrasive treatment with an Al<sub>2</sub>O<sub>3</sub> artificial corundum powder with a particle size of 150–250 μm was performed for 30 s at an excess air pressure of 0.4–0.6 MPa. This preparatory procedure enhances the chemical activity of the metal surface and results in its work hardening due to the formation of a structurally inhomogeneous layer in the process of repeated local microdeformation of the surface by abrasive particles. At the second stage, routine ultrasonic cleaning at an oscillation frequency of 22 kHz was performed to remove process contaminants in the form of residual abrasive microparticles and fatty components.

The experimental alloying coating for laser modification was prepared from graphite paste (GOST 8295-73) and titania (anatase) powder with a particle size of 20–25 nm. The graphite paste and the nanosized titania powder were mixed in a mass ratio of 4:1 to a uniform mass. The alloying composition was then deposited evenly onto the surface of samples. The thickness of the coating layer was 250 ± 50 μm. The TiO<sub>2</sub> powder was used as an additional high-hardness component that enhanced the microhardness of the formed surface.

Two methods for laser hardening of the steel surface were chosen for further comparative analysis:

1. Laser modification of the surface subjected to air-powder abrasive treatment (APAT + LM).
2. Laser modification of the surface, which was subjected to air-powder abrasive treatment, with a coating layer prepared from graphite paste and anatase powder in a mass ratio of 4:1 ((APAT + graphite paste)/(anatase + LM)).

An LRS-50A automated setup for thermophysical coherent surface modification was used to perform pulsed processing of the surface of samples made from stainless chromium-nickel steel 12Cr18Ni10Ti. Energy  $E$  of a single pulse at different voltages was determined experimentally using a LaserStar Ophir (Laser Measurement Group) laser energy and power measurement device.

The following primary control factors were chosen for the experiment: pump lamp voltage  $U$  [V] and diameter  $\phi$  [mm] of laser pulses focused to a spot.

The minimum voltage was 250 V. A slight change in the texture of the scanned surface becomes visible in this mode. The maximum pulse voltage was set to 450 V, since this processing mode gives rise to considerable surface fusion and burning. The pitch of voltage variation of the laser pulse was 50 V in the 250–450 V interval.

The values of energy  $E$  of a single laser pulse were determined experimentally using the laser energy and power measurement device. The duration of pulses ( $\tau$ ) was kept constant at 0.5 ms. The average values characterizing the dependence of the pulse energy on the pump lamp voltage are listed in Table 1.

Two values of diameter of the laser pulse focused to a spot were set: 0.5 and 1 mm. The scanning rate was 20 Hz with a pulse pitch of 0.2 mm.

**Table 1.** Dependence of the pulse energy on the pump lamp voltage

$\tau$ , ms	$U$ , V	$E$ , J
0.5	250	0.08
	300	0.31
	350	0.58
	400	0.92
	450	1.35

The elemental composition was determined by energy-dispersive X-ray fluorescence (EDXRF) using a MIRA II LMU microscope with an INCA PentaFETx3 detector (Oxford Instruments). The elemental composition of the surface was determined based on the spectra of chemical elements within several microregions of the surface. The number of studied local regions varied from 3 to 10. The data on the concentration of specific elements in the modified surface material were averaged after measurements.

X-ray diffraction (XRD) analysis was performed using an ARL X-TRA (Thermo Fisher Scientific) diffractometer with Cu-K $\alpha$  radiation ( $\lambda = 0.15412$  nm) in the  $2\theta$  angle range of 5–90°. The library of the international electronic database of diffraction standards COD-Inorg Rev248644 dated 03.03.2020 in Match Version 1.11 was also used.

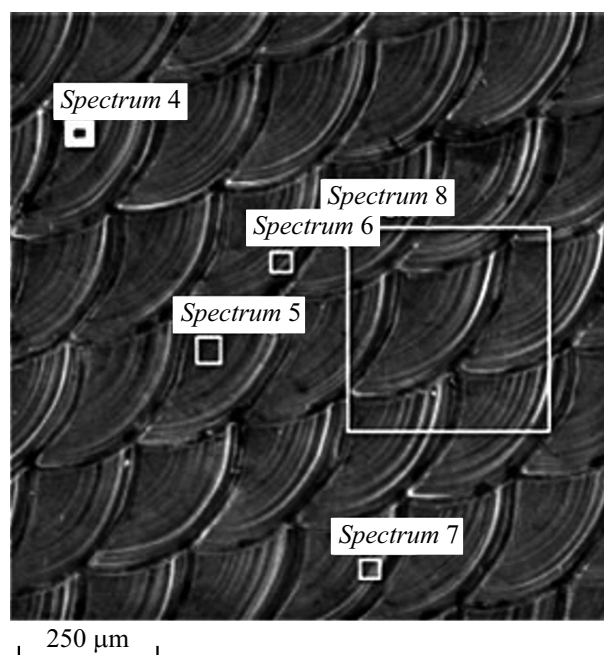
The morphology was studied by scanning electron microscopy (SEM) in the match mode with the elemental composition determined using a MIRA II LMU electron microscope.

The microhardness of the modified surface was determined by the Vickers method with a PMT-3M microhardness meter at a load of 0.981 N on the diamond indenter (GOST 9450-76).

## 2. Results and discussion

Since the most pronounced features of the elemental and phase composition and the morphology of the modified samples were formed at a pump lamp voltage of 400 V with energy  $E = 0.92$  J of laser pulses and a focal spot diameter of 0.5 mm, the results of chemical analysis and XRD and the structures of sample surfaces detailed below correspond to this laser processing mode.

The chemical analysis of the surface of an APAT + LM series sample revealed the presence of such elements as Al and O (Fig. 1, Table 2). These elements are not found in the initial composition of steel 12Cr18Ni10Ti. The presence of trace (up to 1.48 at.%) amounts of aluminum in the surface layer is attributable to the preparatory air-powder abrasive treatment wherein single particles of artificial corundum are embedded into the substrate surface. The enrichment of the surface with oxygen to 7–16.15 at.% is the result of

**Figure 1.** SEM image of the surface of an APAT + LM series sample. The spectra used for EDXRF are indicated.

oxidation of steel in reactive interaction with air oxygen under the thermal influence of laser pulses.

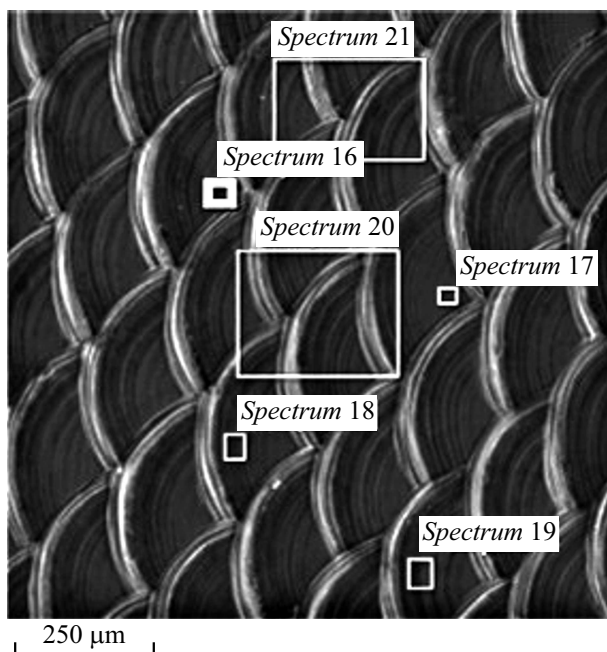
The elemental composition of the modified surface of (APAT + graphite paste)/(anatase + LM) series samples was characterized by a somewhat lower oxygen content (up to 8.5 at.%). This is attributable to the fact that the diffusion of oxygen into the surface of samples under an alloying coating was hindered and reactive oxidation processes were slowed down (Fig. 2, Table 3). The primary contribution to the concentration of oxygen on the surface was produced by TiO<sub>2</sub> particles present in the composition of the alloying coating. In addition, an elevated concentration of carbon (up to  $1 \pm 0.5$  at.%) was noted. This was the result of diffusion of carbon into the surface from graphite with the formation of a cemented layer.

XRD analysis was performed in order to determine the phase composition of the modified surface of steel samples and to estimate its effect on the structure and the characteristics of the surface layer. It was found that the surface layer of samples subjected to the preparatory air-powder abrasive treatment and subsequent laser modification contains austenite ( $\gamma$ -Fe), ferrite ( $\alpha$ -Fe), graphite, and a mixture of metal-oxide compounds forming a heterophase structure (Fig. 3) [16].

Owing to hardening under the thermal influence of laser pulses, the Fe<sub>2</sub>C carbide phase formed as a result of processing. The identification of iron oxide Fe<sub>3</sub>O<sub>4</sub>, chromium oxide Cr<sub>2</sub>O<sub>3</sub>, and titania TiO<sub>2</sub> (in the form of rutile) phases in the obtained XRD pattern is indicative of the process of laser oxidation, which may be regarded as a distinct method for production of thin-layer heterophase coatings with different properties and functional characteristics [17].

**Table 2.** Elemental composition of the surface of an (APAT + LM) series sample, at.%

Spectrum designation	Spectrum 4	Spectrum 5	Spectrum 6	Spectrum 7	Spectrum 8
O	12.46	10.14	6.97	10.25	16.15
C	0.12	0.11	0.8	0.10	0.12
Al	0.63	0.65	0.67	0.91	1.48
Si	1.28	1.46	1.19	1.37	1.75
Ti	0.34	0.35	0.29	0.36	1.09
Cr	19.79	19.97	20.47	20.26	20.07
Mn	0.36	0.38	0.40	0.34	0.47
Fe	57.31	59.36	61.53	58.07	50.95
Ni	7.71	7.58	8.40	8.34	7.97
Total	100.00	100.00	100.00	100.00	100.00

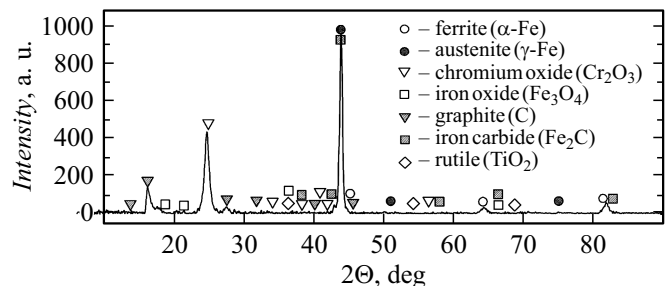
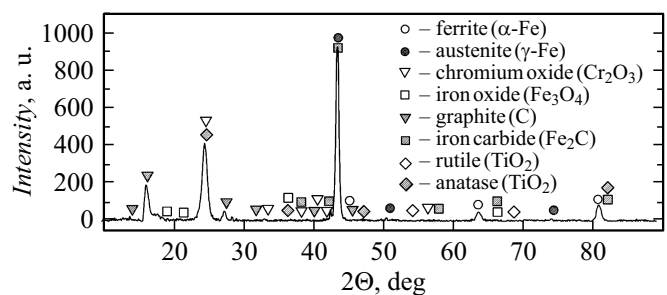
**Figure 2.** SEM image of the surface of an (APAT + graphite paste)/(anatase + LM) series sample. The spectra used for EDXRF are indicated.

It was determined based on the intensity of diffraction peaks and the EDXRF data that chromium oxide  $\text{Cr}_2\text{O}_3$  and the  $\alpha$ -Fe phase constitute the bulk of the formed composition.

Experimental data demonstrate that laser treatment induces the processes of surface hardening and oxidation, which result in the formation of iron carbide and a mixture of metal oxides in the surface layer (Fig. 3).

The results of XRD of (APAT + graphite paste)/(anatase + LM) series samples revealed an increased intensity of austenite and ferrite peaks and iron carbide

(Fig. 4). It was established that the alloying coating hinders the processes of absorption of air oxygen by the surface, which lead to the formation of metal-oxide compounds, and thus suppresses the formation of iron ( $\text{Fe}_3\text{O}_4$ ) and chromium ( $\text{Cr}_2\text{O}_3$ ) oxides. An increased intensity of diffraction peaks of the graphite phase was noted. This is the result of diffusion of carbon from the graphite paste with the formation of a cemented layer. The phase of anatase titania  $\text{TiO}_2$  emerges in the composition

**Figure 3.** XRD pattern of the surface layer of an APAT + LM series sample of steel 12Cr18Ni10Ti.**Figure 4.** XRD pattern of the surface layer of an (APAT + graphite paste)/(anatase + LM) series sample of steel 12Cr18Ni10Ti.

**Table 3.** Elemental composition of the surface of an (APAT + graphite paste)/(anatase + LM) series sample, at. %

Spectrum designation	Spectrum 16	Spectrum 17	Spectrum 18	Spectrum 19	Spectrum 20	Spectrum 21
O	5.55	3.75	4.46	5.00	8.52	7.30
C	0.81	0.76	0.84	0.93	1.05	1.01
Al	0.69	0.25	0.34	0.43	0.80	0.76
Si	1.05	0.99	0.80	0.84	1.20	1.06
Ti	0.53	0.32	0.41	0.62	1.08	1.12
Cr	17.58	18.18	18.00	17.74	17.17	17.37
Mn	0.62	0.56	0.64	0.59	0.59	0.59
Fe	65.26	67.05	66.65	66.05	62.1	63.15
Ni	7.91	8.14	7.86	7.80	7.49	7.64
Total	100.00	100.00	100.00	100.00	100.00	100.00

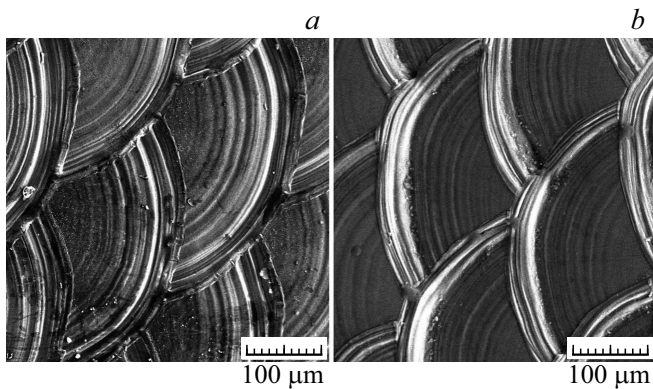


**Figure 5.** SEM images of the surface of samples: *a* – (APAT + LM), *b* – (APAT + graphite paste)/(anatase + LM).

of the modified surface. This stems from the presence of nanosized anatase particles in the composition of the experimental alloying coating.

The morphological alterations of the surface after laser pulsed processing were analyzed using scanning electron microscopy. It was found that the surface microstructures obtained with each method of laser modification were somewhat similar (Fig. 5), but differed slightly in the cell structure of produced spots. For example, a large number of microparticles formed near the center of spots in the sample without the alloying coating (Fig. 5, *a*). Such clusters of crystallized particles were not observed at the periphery of spots. The opposite effect was noted in the examination of the sample with nanosized anatase present in the alloying coating. Microparticles were clustered at the periphery of spots in this case (Fig. 5, *b*).

If one examines the surface regions at the periphery of a spot, a quasiperiodic wave relief becomes apparent in these regions. This wave-like microrelief is the result of movement

of the melt in the radial direction from the center toward the edge induced by the shock action of a laser pulse. This effect is intrinsic to all such regions of the scanned surface of test samples. The obtained results suggest that the use of the alloying coating contributes to an increase in periodicity of formation of thermocapillary waves and to their flattening.

The APAT + LM series sample was, on the contrary, characterized by a greater pitch between neighboring waves and deeper grooves at their boundaries. This difference is attributable to the capacity of the coating to absorb a fraction of energy of the heat flux of a laser pulse.

Higher-magnification examination of the modified surface at the periphery of spots revealed that nanometer crystals with an average size of 30–100 nm, which form dense clusters of nanoparticles, are the primary structural component in these regions (Fig. 6). The formation of nanosized cracks on the surface of the APAT + LM series sample was noted. This is attributable to an increase in internal stress in the surface layer in the process of scanning without the alloying coating (Fig. 6, *a*). It was found that the nanostructure

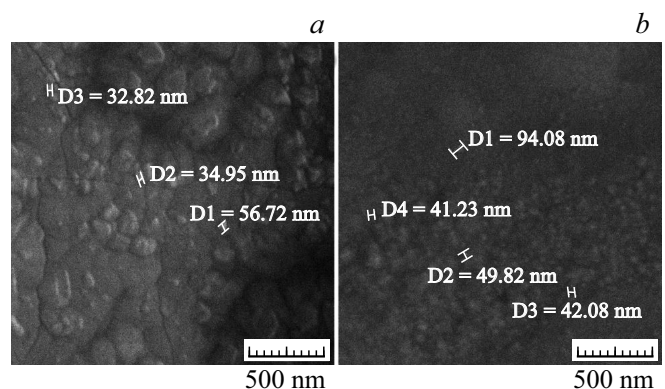


**Figure 6.** SEM images of the surface of samples at the periphery of spots: *a* – (APAT + LM), *b* – (APAT + graphite paste)/(anatase + LM).

**Table 4.** Average values of microhardness of test samples of stainless steel 12Cr18Ni10Ti

Processing technique	LM modes			Surface microhardness	
	$\varnothing$ , mm	$U$ , V	$E$ , J	HV	H, GPa ( $\pm 0.1$ )
APAT + LM	0.5	250	0.08	297	2.91
		300	0.31	347	3.4
		350	0.58	275	2.7
		400	0.92	394	3.86
		450	1.35	–	–
	1	250	0.08	681	6.68
		300	0.31	365	3.6
		350	0.58	306	3.01
		400	0.92	420	4.12
		450	1.35	466	4.57
(APAT + graphite paste)/(anatase + LM)	0.5	250	0.08	309	3.03
		300	0.31	465	4.61
		350	0.58	491	4.83
		400	0.92	921	9.03
		450	1.35	–	–
	1	250	0.08	509	4.99
		300	0.31	343	3.36
		350	0.58	409	4.01
		400	0.92	261	2.56
		450	1.35	273	2.39

formed with the use of the alloying coating had highly uniform and ordered morphological elements (Fig. 6, b).

The obtained SEM data are indicative of the formation of different types of surface morphology of test steel samples with distinctive features of structuring at the center of produced spots and at their periphery where a quasiperiodic relief typically forms. The APAT + LM series samples were characterized by a greater pitch between thermocapillary waves at the periphery and deeper grooves at their boundaries (Fig. 5).

In general, SEM images revealed the formation of nanocrystals, which has a size of 20–50 nm at the spot center (near the crater) and grew slightly to 50–70 nm toward the periphery, on the modified steel surface. It follows from scientific and technical literature data that the formed nanosized crystals are both highly thermally stable and may contribute to a considerable enhancement of the mechanical strength, the impact strength, and other characteristics of a surface subjected to laser modification [18].

The microhardness of surfaces of samples of two test series was determined. It was found that the microhardness of samples with the experimental coating deposited on them and subjected to laser processing by pulses focused to a spot 0.5 mm in diameter was 100–150 HV higher than that of samples modified without the coating layer under the same parameters of laser treatment (Table 4). A different hardening effect was observed for a focal spot diameter of 1 mm. The microhardness of the surface of samples without the coating was somewhat higher in this case. This is attributable to the fact that the concentration of energy in a spot 1 mm in diameter is not sufficient to heat the surface, since the released heat is absorbed partially by the coating.

It should be noted that the microhardness of the surface treated with laser pulses focused to a spot 0.5 mm in diameter at a voltage of 450 V could not be measured due to intense surface fusion and the formation of chaotically arranged macroparticles and a rough highly porous structure on the surface.

The obtained experimental data were averaged and tabulated. The numerical values of microhardness of the modified surface determined for different modes and techniques of laser pulsed treatment are presented in Table 4.

## Conclusion

The process of laser pulsed modification of the surface of samples made from chromium-nickel steel 12Cr18Ni10Ti and subjected to preparatory air-powder abrasive treatment was studied. Two methods of modification (with an without the application of experimental alloying coating made from graphite paste and nanosized anatase titania  $\text{TiO}_2$  particles) were tested.

EDXRF studies of the elemental composition showed that the samples modified without the coating contained, in addition to the base chemical elements of steel 12Cr18Ni10Ti, Al and O. The concentration of impurity aluminum, which comes from the  $\text{Al}_2\text{O}_3$  artificial corundum powder used in the preparatory air-powder abrasive treatment, on the surface was low (up to 1.48 at.%). The oxygen content was 7–16.15 at.%. This oxygen is the result of oxidation processes during laser scanning. The oxygen content of the surface of samples modified with the alloying coating was somewhat lower (up to 8.5 at.%). The primary contribution to this concentration was produced by titania ( $\text{TiO}_2$ ) particles found in the composition of the coating. An elevated concentration of carbon ( $1 \pm 0.5$  at.%), which formed a cemented layer of the surface of samples due to diffusion from the graphite paste, was found.

The XRD studies revealed that the surface layer of steel samples subjected to laser treatment without the coating contains austenite ( $\gamma$ -Fe), ferrite ( $\alpha$ -Fe), graphite, carbide  $\text{Fe}_2\text{C}$ , and a mixture of metal-oxide compounds  $\text{Fe}_3\text{O}_4$ ,  $\text{Cr}_2\text{O}_3$ , and  $\text{TiO}_2$  (rutile).

It was established that the application of alloying coating results in a reduction in the concentration of phases of iron

and chromium oxides and an increase in the concentration of iron carbide and graphite. Since anatase titania  $\text{TiO}_2$  is present in the graphite paste, it is also present in the composition of the modified surface.

The results of comparative electron-microscope analysis of the modified surface of stainless steel with and without the experimental coating revealed that different surface structures with distinctive features of structuring at the center of produced spots and at their periphery form under laser pulsed scanning. The study of morphology of individual spots showed that nanometer particles with an average size of 20–50 nm are the major component in the center area of spots. Pronounced thermocapillary waves formed closer to the periphery of spots. The use of the alloying coating contributed to an increase in their periodicity and to their flattening with the formation of a smoother surface microrelief. The size of particles at the periphery of spots is 50–70 nm, and the surface structure of samples scanned with the coating layer is more even and homogeneous.

The microhardness of test samples was determined, and it was found that the alloying coating enhances it considerably. Specifically, the microhardness of the surface modified with the coating deposited on it was 100–150 HV higher than that of the surface modified without the coating layer and reached a maximum of 921 HV. It was also found that the microhardness enhancement associated with the use of the experimental coating is achieved when laser pulses are focused to a spot 0.5 mm in diameter. If the spot diameter is 1 mm, the heating of the modified surface is not sufficient due to the weak concentration of heat in the focal area and absorption of a fraction of thermal energy by coating components. Hardening structures form in the surface layer in these conditions, producing a mixed composition of mechanically strong phases of graphite,  $\text{Fe}_2\text{C}$ ,  $\text{Cr}_2\text{O}_3$ , anatase  $\text{TiO}_2$ , and  $\text{TiO}_2$  (rutile).

## Funding

This study was supported by a grant from the Russian Foundation for Basic Research (contest „Postgraduates“ for the best projects in fundamental research conducted by young postgraduate students), project No. 19-33-90101.

## Conflict of interest

The authors declare that they have no conflict of interest.

## References

- [1] M. Moradi, D. Ghorbani, M.K. Moghadam, M. Kazazi, F. Rouzbahani, Sh. Karazi. *J. Alloys Compounds*, **795**, 213 (2019). DOI: <http://dx.doi.org/10.1016/j.jallcom.2019.05.016>
- [2] M. Moradi, H. Arabi, S.J. Nasab, K.Y. Benyounisc. *Optics Laser Technol.*, **111**, 347 (2019). DOI: 10.1016/j.optlastec.2018.10.013
- [3] J. Sundqvist, T. Manninen, H.-P. Heikkinen. *Surface Coatings Technol.*, **344**, 673 (2018). DOI: 10.1016/j.surfcoat.2018.04.002
- [4] N. Maharjan, W. Zhou, N. Wu. *Surface Coatings Technol.*, **385**, 125399 (2020). DOI: 10.1016/j.surfcoat.2020.125399
- [5] B. Zhang, H. Wang, R. Chen, B. He, Y. Cao, D. Liu. *Surface Engineer.*, **37** (5), 1 (2020). DOI: 10.1080/02670844.2020.1840758
- [6] M. Kulka, D. Mikołajczak, N. Makuch, P. Dziarski, D. Przes tacki, D. Panfil-Pryka, A. Piasecki, A. Miklaszewski. *Materials*, **13** (21), 4852 (2020). DOI: 10.3390/ma13214852
- [7] J. Boes, A. Röttger, W. Theisen. *Additive Manufacturing*, **32**, 101081 (2020). DOI: 10.1016/j.addma.2020.101081
- [8] V.S. Golubev, A.I. Mikhlyuk, I.A. Romanchuk, L.I. Protskevich, in *Proc. XIII Int. Conf. „Modern Methods and Technologies to Create and Process Materials“*, Minsk, 2018, p. 58 (in Russian).
- [9] T. Yamaguchi, H. Hagino. *Vacuum*, **155**, 23 (2018). DOI: 10.1016/j.vacuum.2018.05.050
- [10] F. Laroudie, C. Tassin, M. Pons. *J. Mater. Sci.*, **30**, 3652 (1995). DOI: 10.1051/jp4:1994415
- [11] B. AlMangour, D. Grzesiak, J. Yang. *J. Alloy. Comp.*, **706**, 409 (2017). DOI: 10.1016/j.jallcom.2017.01.149
- [12] I.Y. Khalfallah, M.N. Rahoma, J.H. Abboud, K.Y. Benyounis. *Optics Laser Technol.*, **43** (4), 806 (2011). DOI: 10.1016/j.optlastec.2010.11.006
- [13] D.I. Adebisi, T. Fedotova, S.L. Pityana, A.P.I. Popoola. *Intern. J. Phys. Sci.*, **6** (14), 3336 (2011).
- [14] V.P. Biryukov, *Fotonika*, **27** (3), 34 (2011) (in Russian).
- [15] F. Colville. *Photovoltaics Intern.*, **5** (6), 1 (2009).
- [16] A.A. Fomin, M.A. Fomina, V. Koshuro, I.V. Rodionov. *Composite Structures*, **229**, 111451 (2019). DOI: 10.1016/j.compstruct.2019.111451
- [17] M.A. Vasilyev, I.N. Makeeva, P.A. Gurin, *Usp. Fiz. Met.*, **20** (2), 310 (2019) (in Russian). DOI: 10.15407/ufm.20.02.310
- [18] A. Chirkov, *Fotonika*, **4**, 28 (2008) (in Russian).